**JOURNAL OF ALGEBRAIC STATISTICS**
Volume 13, No. 1, 2022, p. 665-681
https://publishoa.com
ISSN: 1309-3452

# Hybrid Color Image Demosaicking using Densely Connected Residual Sub-pixel CNN with Iterative Ring Resonator-based Gaussian Filter

**Chatla Raja Rao**[*1]**Soumitra Kumar Mandal**[2]
[1]Research Scholar, Department of Electrical Engineering, Maulana Abul Kalam Azad University of Technology, Kolkata, West Bengal, India
[2]Professor, Department of Electrical Engineering,National Institute of Technical Teachers' Training and Research, Kolkata, West Bengal, India
*** Corresponding author's Email:** chatlarajarao25@gmail.com

**Received:** 2022 March 15; **Revised:** 2022 April 20; **Accepted:** 2022 May 10.

**Abstract**
Digital camerasare essential devices in current digital era, where all the cameras capture the images using color filter array (CFA) approach. Usually, while capturing an RGB image, only one color is stored in the pixel and remaining two colors will be missed. Thus, these missed colors in that position must be restored to the fully coloured image, which is referred as the concept of demosaicking. This article focuses on development of advanced demosaicking using deep convolutional neural network (D-CNN) model with self-ensemble method to reduce the computational complexities. The proposed D-CNN model consisting of densely connected residual blocks with the densely connected residual network (DRDN) for the training of various mosaic patterns and CFAs. Thus, this architecture reduces the vanishing-gradient problems generated during the training process with the utilization of efficient sub-pixel convolutional neural network (ESPCN) layer. The test images are applied to the D-CNN+DRDN architecture and performs the initial demosaicking operation using the local features of block-wise convolutional layers. Finally, iterative ring resonator based Gaussian filter (IRRGF) method is employed to generate the high intensity output demosaicked image. Extensive simulation results shows that proposed hybrid color image demosaicking model gives the enhancive subjective and objective performance with least mosaic pattern effects and reduced color errors. Performance evaluation compared to the demosaicking approaches from the literature like DDEMO, DRDN, and DRDN+ in terms color peak signal-to-noise ratio (CPSNR), and structural similarity (SSIM) index.
**Keywords:** Color filter array, demosaicking, deep learning, convolutional neural networks, densely connected residual network, Gaussian filter.

## 1. Introduction

Demosaicking has become very popular among a huge range of people in signal processing as well as applied mathematics. Demosaicking protocols adopt variety of signal processing methods [1, 2] such as inverse problems, neural network, wavelet, Bayesian statistics, and convex optimizations and so on. An outline of

**JOURNAL OF ALGEBRAIC STATISTICS**
Volume 13, No. 1, 2022, p. 665-681
https://publishoa.com
ISSN: 1309-3452

various methods for demosaicking is presented here. The protocols are broadly sorted into a couple of groups as per the progression of protocol development in the domain. As a cost-effective way to capture color images, most digital cameras employ a single monochromatic image sensor, in combination with a CFA [3] placed directly in front of the sensor array; the CFA performs a spatial subsampling procedure, in which every pixel in the array records one portion of the incoming light spectrum. CFA consists of an array of color filters, arranged in a specific manner for sampling one color band at every pixel location. The most used CFA pattern is Bayer pattern, in which red and blue values are sampled on rectangular lattice whereas green value is assessed on quincunx lattice, twice as many as that of red or blue value. Reason for having dense green samples in the CFA pattern is that green filters have spectral responses closer to luminance responses of human visual systems, recording the greatest amount of spatial data is useful for perceived image quality. Spectrally selective filters mosaic and minimal repeating CFA are also called CFA pattern. Usually, formed CFA patterns need not be rectangular. A rectangular CFA pattern [4] is represented by various $2 \times 2$ patterns as shown in Figure 1. Bayer CFA pattern is a popular technique used by sensor manufacturers where the sensor is coated to record one of three color components in each pixel location. Bayer filter mosaics are CFAs for ordering RGB color filters on square grids of photo sensors. Most of the single-chip digital image sensors that are used in digital cameras, camcorders, and scanners utilize the particular arrangement of color filters to create a color image. Thus, the Bayer color filter pattern holds 50% green, 25% red and 25% blue and its various permutations would be GBRG, GRBG, or RGGB and BGGR as shown in Figure 1. Digital cameras embed a series of signal processing operations in their processors to produce images, which is called an image processing pipeline. An image pipeline design plays a key role in digital camera systems for generating high quality images. Although the sequence of operations differs from manufacturer to manufacturer, a general image pipeline consists of a series of processing functions.

In typical digital camera pipeline architecture, the color demosaicking (CDM) [5] is one of the first operations performed after CFA image acquisition. The demosaicked RGB images are then modified by adjusting white balance and performing color and gamma correction to match the colors of the input scene when rendered on a display device. White balancing operation makes the white objects appear as white by removing the color tint of an image. Color correction converts the CFA sensor color space to a standard RGB space, such as linear RGB. Gamma correction adjusts the image intensity to manage the nonlinearity of CRT or LCD display. Once adjustment and correction processes are completed, the enhanced image is compressed for storage or transmission. Moreover, noise may also be present because of communication errors or compression.Hence, de-noising is typically required and is the first stage prior for analysis of image data. It is required to employ effective de-noising method for compensating the corruption of data. Image de-noising is a huge problem for most research scholars as removing noises brings about artifacts apart from blurs in the image. Almost all digital color cameras currently utilize single sensor with CFAs for capturing visual scene in color.

**JOURNAL OF ALGEBRAIC STATISTICS**
Volume 13, No. 1, 2022, p. 665-681
https://publishoa.com
ISSN: 1309-3452

The presence of noise in CFA information leads to deterioration of visual quality of acquired images apart from extreme demosaicking artifacts that is hard to eliminate through consequent de-noising procedure. An immense number of demosaicking methods have been proposed in the literature.

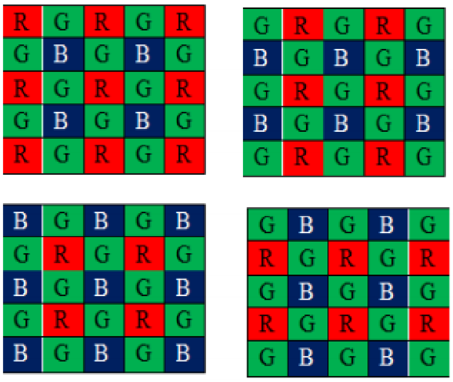


**Figure 1: Different forms of Bayer mosaic patterns.**

Rest of the paper organized as follows: Section 2 contains an elaborative study of existing literature on CFA Demosaicking methods. The Section 3 describes the proposed CFA demosaicking architecture which employs IRRRGF method. Section 4 deals with the experimental analysis using standard datasets and comparative analysis with various state-of-art approaches. Section 5 concludes the paper with possible future enhancements.

## 2. Related work

Basic Demosaicking algorithms employed for interpolation of missing colour samples in CFA image are nearest neighbour [6], bilinear [7], or bicubic interpolation [8] algorithms. However, these simple interpolations resulted in many false color artifacts such as blurring, chromatic aliases, zippering, and purple fringing [9] etc. To overcome these problems many interpolation-based approaches are presented in the literature. The approaches are four-direction residual interpolation for demosaicking (FDRI) [10], adaptive residual interpolation for demosaicking (ARI) [11], multi gradients-based demosaicking (MSG) [12], edge strength filter based demosaicking (ESF) [13], directional filtering and weighting (DDFW) [14], directional linear minimum mean square error estimation (DLMMSE) [15], matrix factorization iterative tunable (MFIT) [16], LMMSE [17] and Markov based image forgery detection (MIFD) [18]. In [19] authors focused on the classification of color textures obtained by single sensor color cameras by using RGBW CFA approach. In those cameras, RGBW CFA makes every photo sensor sensitive to solely one-color elements, and CFA images are to be demosaicked to predict the final color images. The authors showed that demosaicking is degrading to the textural data as it impacts color texture descriptors like chromatic co-occurrence matrices (CCMs). In [20] authors proposed to create a pair of quarter-size color images directly from second order statistical (SOS) analysis for CFA images without any prediction, then to calculate the CCMs of the quarter-size images. Outcomes of experiments performed on benchmark color textural datasets showed the efficacy of the suggested method for textural classification while complexity studies highlight the computation efficacy.

To overcome the above stated issues, deep learning architectures were adopted for the demosaicking operation. In [21] authors proposed a novel quality-efficient universal demosaicking for arbitrary CFA using sparse based radial basis function (SRBF). In their proposed method, both the spatial and the temporal correlations among the CFA data are taken into account during the demosaicking. Then an effective least square-based approach

**JOURNAL OF ALGEBRAIC STATISTICS**
Volume 13, No. 1, 2022, p. 665-681
https://publishoa.com
ISSN: 1309-3452

was developed to fuse the spatial-based demosaicked result and the temporal-based one. In [22] authors presented a novel iterative denoising and demosaicking technique with CNNs as well as the color shrinkage using repetitive color transform. The novel CNN-demosaicking technique was initially created for the Bayer's primary CFA, but a slight alteration enables its application in several CFAs apart from the Bayer one. In [23] authors proposed deep residual learning (DRL) and applied it to the demosaicking issue. MDFCN output was used for improving initial green channel interpolation as well as for applying constant color difference rule in an adaptive manner. The MDFCN directed technique produces visually pleasing outcomes with poorer CPSNR. A 2-layer CFA to obtain high quality image as well as demosaicking protocols for interpolating a suggested generative adversarial network (GAN) has been proposed by authors [24]. Research results showed performance saturation as color channels sub-sampling is inevitable. To offset this, multilayer CFA has been developed to get 2 or 3 color data at a single pixel position. Simple demosaicking algorithms are presented to evaluate the proposed method's performance. In [25] authors proposed a classified-based D-CNN compensation protocol for CFA demosaicking, which has been utilized for enhancing the image quality of D-CNN outcome acquired by other CFA images. Firstly, all pixels are sorted as per their neighbourhood textural variance as well as angels. Then, various least mean square filters are trained to adopt for handling pixels of several features. In [26], authors presented learning deep convolutional networks scheme of CFA synthesis in digital images through dictionary re-demosaicking. This refers to an anti-forensic method to be against a plurality of forensic techniques on the basis of CFA structure identification in images. Firstly, through sparse abstraction on manipulated images, a dictionary is acquired. In [27], authors presented random CFA demosaicking strategies were permitted to re-demosaicking every dictionary using residual learning. Finally, the image has been reconstructed through the re-demosaicked dictionary. Outcomes from experiments demonstrated that both satisfied image quality with regard to PSNR and stronger CFA characteristic are attained. In [28], authors addressed a method for carrying out image resizing through usage of multiple deep fully convolutional network protocol called as DDEMO. Experiments showed that the method is dependable while performance in image resizing is better than few combined demosaicking as well as zooming protocols and other famous resizing protocols like the CNN algorithm. To overcome these issues, this article focuses on development of advanced demosaicking using D-CNN model with self-ensemble method to reduce the computational complexities. The proposed D-CNN model consisting of densely connected residual blocks with DRDN for the training of various mosaic patterns and CFAs. Thus, this architecture reduces the vanishing-gradient problems generated during the training process with the utilization of ESPCN layer. The test images are applied to the D-CNN+DRDN architecture and performs the initial demosaicking operation using the local features of block-wise convolutional layers. Finally, IRRGF method is employed to generate the high intensity output demosaicked image.

**JOURNAL OF ALGEBRAIC STATISTICS**
Volume 13, No. 1, 2022, p. 665-681
https://publishoa.com
ISSN: 1309-3452

## 3. Proposed Methodology

The proposed DRDN based DCNN layered architecture is presented in Figure 1; it is developed based on the concepts of ResNet [30] and DenseNet [31]. The both networks will be effectively used to identify the mosaic problem and identify the missing pixels with the suppression of vanishing-gradient problems occurred in conventional approaches. Then, DRDN takes the responsibly to restore the missing pixel with the help of trained database. The input applied to the DCNN model contains only quarter of test input size, thus the DCNN model takes less time for training and testing operations. As the size of the input reduces, then the requirement of Neurons and feature maps also reduced, thus input memory stored into feature maps also reduced effectively. It indicates that the proposed model utilized low memory and computational complexities are also reduced.

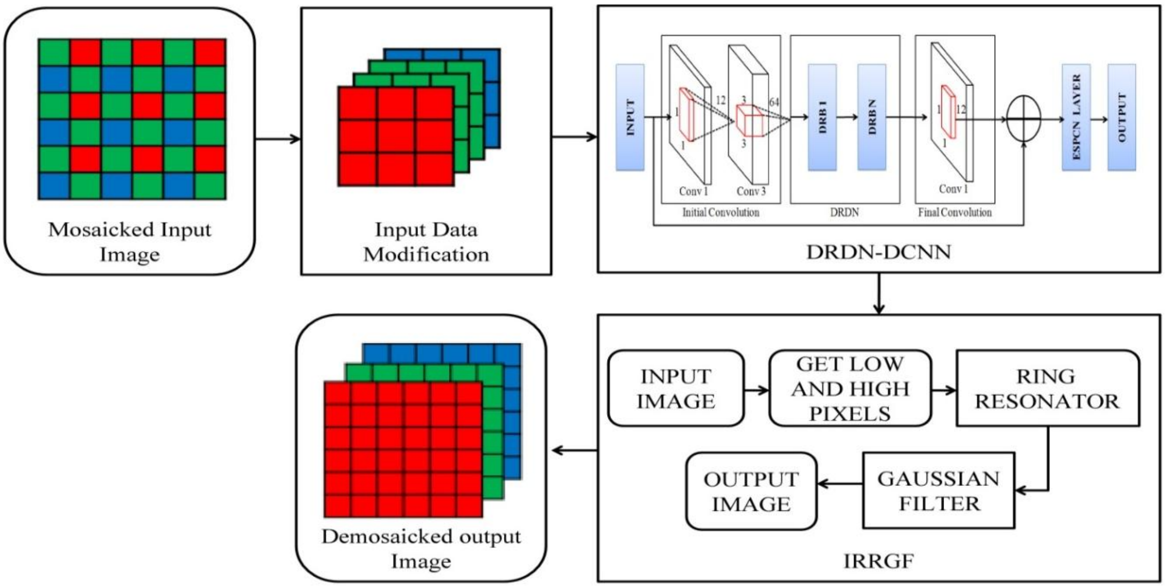


**Figure 2: Flow of the proposed demosaicking approach.**

The DRDN based DCNN network is trained with the various mosaic patterns with different CFAs. So, when test image is applied, its color filters are analyzed, and mosaic patterns are extracted by DRDN effectively. Then, DCNN applies the mosaic removal operations and results in prominent demosaicked out image. But the resultant output image does not contain the same resolution as original mosaicked input image. To solve this, our network applies the ESPCN layer to demosaicking solution, which generates the high-resolution output image. The proposed ESPCN layer learns an up-scaling filter to upscale their final output. This enables the network to reduce the computational complexity also. Then, SEM is employed, which shows significant performance enhancement without additional time or computational complexity consumptions. However, the multi-layer structure costs a lot of time and computational complexity, as it needs to train additional networks. On the other hand, the self-ensemble method, which averages the outputs of the transformed input images, only needs one trained network. By applying SEM, the performance of our proposed network gets increased without training additional networks. Finally, IRRGF method is applied to convert low intensity pixels to high intensity pixels. This method is used to generate demosaicked images more efficiently and accurately with perfect smoothing.

The architecture of various blocks of the proposed model are explained below.

### 3.1. DRDN-based DCNN architecture

The DRDN based DCNN architecture consisting of four major parts; they are initial convolution block, densely connected residual blocks (DRBs) [32], final convolution layer, and ESPCN layer [33]. The proposed DL-CNN architecture consisting of densely connected residual blocks (DRBs) and convolution layers for providing the better accuracy compared to the other state of art approaches.By using the circular transformation, the real valued test features are converted to complex domain. Different layers are used to perform the one-to-one mapping of these real-valued features, the complex domain data is generated in all four quadrants by this transformation. The convolution layer contains the hyperbolic secant activation function with Gaussian-like search operation. Finally, the system of linear equations is generated by this approach with the effective utilization of Optimal output weights.Thus, these weights are applied to the ESPCN layer through the orthogonal assessment regions and the resolution matching will be achieved.

DRDN is the neural network with several feature processing layers. The convolutional layers are used to apply the filters with various sizes on the test images. The convolution layers are using the bias $b_k$ and filter $W_k$ at k$^{th}$ stage. Then apply those filers on input at $i$ location, thus the resultant output generated at location $j$ as expressed below,

$$Y_k(j) = \sigma\left(\sum_{i \in \Omega(j)} X_{k-1}(i) * W_k(i,j) + bkj\right) \quad (1)$$

Here, mainly $X(j)$ denotes the input image and $Y(j)$ denotes the output image, $*$ denotes the convolution operation, and finally a ESPCN function is denoted by $\sigma(.)$ . Here, $\Omega(j)$ denotes the region of input image and its values are pooled by sub sampling function. Figure 3 presents the detailed schematic diagram of proposed DRDN based DCNN architecture with global residual learning procedure.

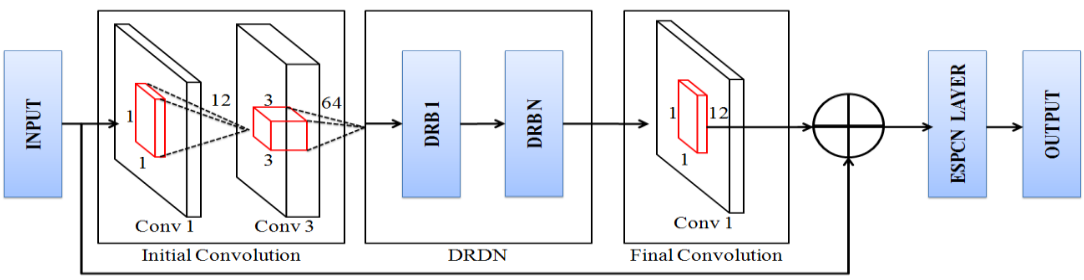


**Figure 3: Global residual learning architecture of the proposed method.**

**JOURNAL OF ALGEBRAIC STATISTICS**
Volume 13, No. 1, 2022, p. 665-681
https://publishoa.com
ISSN: 1309-3452

The detailed description of proposed DCNN architecture with each layer operation as follows:

- CONV 1 layer is used to calculate the neurons output, which is interconnected to the local region in input image. Here, 12 feature mapsare used to generate the weight coefficients and each neuron performs a dot product operation between the weights to the small, interconnected region or pixels of input image. Finally, the size of the CONV 1 layer developed as [$1 \times 1 \times 12$]. CONV 1 layer will identify the mosaic patterns with its size. The mosaic patterns will be initially identified to perform demosaicking operation.
- CONV 3-layer functions same as CONV 1 layer and it is also used to generate the activation function and performs the element wise operation with maximum thresholding at zero. Thus, the size of the layer will remains changed such as [$3 \times 3 \times 64$]; Here 3 indicate width and height of filter size and 64 indicates feature maps,respectively. CONV 3 layer is majorly responsible for removing the color errors, readjusting the color levels, Mosaic patter identification and pixel level mosaic correction to generate demosaicking output image.
- DRB layers are used to perform the multi-layer convolution operation with various feature maps and filter sizes.
- Finally, the ESPCN layer generates demosaicked images with the desired resolution. This layer consisting of the multiple up sampling and down sampling filters. By performing the sub sampling operation between the input to the filters, output image generated with required resolution.

### 3.2. Densely connected residual block

The proposed local residual learning architecture of DRDN as shown in Figure 4 consisting of numerous convolutional layers is categorized into convolution blocks and a transition layer, respectively. Convolutional layers are majorly responsible for removing the color errors, readjusting the color levels, Mosaic patter identification and pixel level mosaic correction to generate demosaicking output image. Totally three convolution blocks and one transition layer block respectively, output of each block is connected to another block in densely connected manner. The convolutional block consisting of CONV1 with filter size [1, 1, k] and CONV3 layers with filter size [3, 3, 4k].

Here, k indicates the feature maps, so the CONV3 layer generates the four times higher maps compared to the CONV1 layer, respectively. After each convolution block, RELU based activation function is used for accurate feature mapping. Here, the red, green, and blue lines are indicating these activation functions. Finally, transition layer is used with the convolutional layer by the filter size [1, 1, and 64], here 64 indicates the feature size. The transition layer is used for the effective reconstruction of color errors. Finally, to maintain the size of output image and to generate the enhancive outcome exclusive or operation is performed between convolution al inputs to the transition layer output.

**JOURNAL OF ALGEBRAIC STATISTICS**
Volume 13, No. 1, 2022, p. 665-681
https://publishoa.com
ISSN: 1309-3452

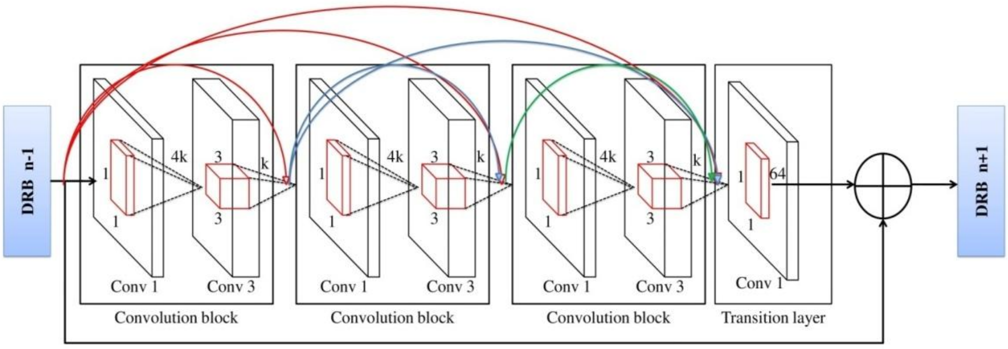


**Figure 4: Local residual learning architecture of DRDN.**

This method is used to perform the conversion of weak intensity pixels to high intensity pixels. For performing this conversion all the input image pixels are iterated and its intensity value will be evaluated and further adjusted for smoothing operation. The block diagram of IRRGF method is presented in Figure 2 and algorithm is presented in Table 1, respectively. The detailed operations of IRRGF approach as follows:

- The input image is applied to the IRRGF method. By pixel value is extracted by using iterative process from the row ($x$) and column($y$).
- Then introduce the smoothing coefficient $d_{xy}$ and iterative coefficient$N_{xy}$. By using these coefficients, the pixel colour values, and intensity levels will be extracted.
- On the extracted colour intensities, apply the ring resonator. It will iterate the pixels in different modes, they are initially it will keep rows as constant and iterates the column pixels with fixed distance. And then it will keep columns as constant and iterates the row pixels with fixed distance. Then, both diagonal movement of row pixels and column pixels are iterated. Finally, all the rows and column pixels are iterated in chronological order. Among all these iterations, weak pixels of RGB mosaic layers are identified easily. During the iteration process, multiple high intensity local pixels are identified based on the nearest values, respectively.
- Finally, Gaussian filter applied with sigma as unity on high intensity local pixels standard mean properties. This Gaussian filter performs convolution operation between high intensity local pixels to the kernel function, respectively. Then the resultant outcome will be generated and replaces the value of original weak pixel location, respectively.
-

**Table 1. IRRGF algorithm.**

| **Algorithm 1: IRRGF** |
|---|
| Input: L (low intensity image), Output: H (High intensity image) |
| **Step 1:** Extract the pixel values. Pixel = $L(x,y)$ |
| **Step 2:** Extract the low and high pixel values in $x,y$ directions. |
| $C_x$=Reshape (pixel [0]-0.5*$d_{xy}$, pixel [0] + 0.5*$d_{xy}$, $N_{xy}$) |
| $C_y$= Reshape (pixel [1]-0.5*$d_{xy}$, pixel [1] + 0.5*$d_{xy}$, $N_{xy}$) |
| **Step 3:** Perform the iterative ring resonator operation. |
| Local [x, y] = ring resonator d ($C_x, C_y$) |
| **Step 4:** Apply the mean Gaussian filter to generate the high intensity pixels. |
| H=mean (Gaussian filter (local [x, y], sigma=1) |

JOURNAL OF ALGEBRAIC STATISTICS
Volume 13, No. 1, 2022, p. 665-681
https://publishoa.com
ISSN: 1309-3452

Most of the existing CNN algorithms consisting of the train dataset image clustering, initial demosaicking with interpolation and training as its substantial pre-processing blocks. They utilized the Initial interpolation block for maintaining the output image resolution size same as the original test image. And they used CNN with multiple layers for maintaining the resolution of output, but at a cost of maximum unwanted memory usage with the higher computational complexity. As the size of the output image is increases the computational complexity of these methods will increase. Most of the methods cluster the training dataset, thus the system needs to train each and every cluster, and this phenomenon naturally increases the computational complexity. As recorded in the outcomes of deep learning approaches, the strategies could considerably enhance image quality; additionally, better visual perceptual may be got. It is to be noted that the suggested technique is regarded as efficient post-compensation through the application for any earlier strategies for yielding even better image qualities. To solve the problems of conventional CNN algorithms, the proposed CFA demosaicking approach is developed using the DRDN presented in Figure 2. And, to reduce the computational complexities generated due to Initial interpolation and initial demosaicking operation will be replaced by input data modification stage in the proposed method. Table 2 presents the detailed algorithm of the proposed method.

**Table 2: Proposed DRDN+ IRRGF algorithm.**

| |
|---|
| Input: Mosaicked input image, Output: Demosaicked output image |
| Step 1: Train the neural network with different mosaic patterns with various CFA. |
| Step 2: Divide the input image into four color layers based on Bayer mosaic patterns. |
| Step 3: Apply the DRDN based DCNN architecture to perform the demosaicking operation with lower computational complexity. |
| Step 4: Apply the ESPCN layer to generate the demosaicking image with same resolution of input image. |
| Step 5: Perform the self-ensemble method (SEM) for performance enhancement for better visual and objective outcomes. |
| Step 6: Finally, IRRGF method was applied to convert low intensity pixels to high intensity pixels with the use of Gaussian filter. |
| Step 7: it results in final demosaicked output image. |

The Mosaicked input image is applied to the input data modification stage**.** Here, the four-color layers are generated with the two green layers, one blue layer and one red layer respectively, thus the size of input is reduced to quarter. Here, the numbers of blue layers are increased compared to the other layers, because the atmospheric light contains higher blue color properties and the Bayer mosaic patter also contains the greener pixels as compared with red, blue pixels (as presented in Figure 1). Eventually, existing demosaicking approaches used interpolation, thus the green layers are not extracted properly at a cost of high computational complexity. Whereas the proposed input data modification method utilizes the simple color rearranging process, thus the green pixel will be separated effectively, and layer formulation achieved with least computational complexity. Then, the DRDN based DCNN is used to train the network with different Mosaic patterns. Output

**JOURNAL OF ALGEBRAIC STATISTICS**
Volume 13, No. 1, 2022, p. 665-681
https://publishoa.com
ISSN: 1309-3452

from the input data modification stage with R, G, G, and B color layered images are applied as input to the proposed network.

## 4. Results and discussion

In this section, the performance of the proposed network with simulation experiments is demonstrated. The network training is carried out under the TensorFlow environment, which is installed on a PC with Nvidia GeForce® MX250 GPU and Intel Core i5-8265U CPU. The training sets are created beforehand and then uploaded into TensorFlow.

### 4.1. Dataset

As many image processing solutions that apply CNN architecture have been proposed, many datasets have been used for training networks. The DIV2K training and validation datasets include high quality images. The DIV2K training dataset consists of 800 images where the resolution of each image is similar to the FHD resolution $(1920 \times 1080)$ [34]. The DIV2K validation dataset consists of 100 images, where the resolution of each image is similar to the training dataset. Given the high quality of the images in the DIV2K, many state-of the-art image processing methods use this dataset and show improved performance. Thus, we train our proposed network with the DIV2K training and validation sets. When training our network, we use patches that are extracted from the training dataset where the width and height of the patches are set to 64 pixels. To augment the training patches, we randomly rotate and flip the input patches before entering the proposed network. We set the batch size of the training patches to 64 and train our proposed network for 300 epochs. We use the Adam optimizer with an initial learning rate of $10^{-4}$ and divided it by 10 for every 100 epochs. For the activation function, we used the leaky rectified linear unit (leaky ReLU), where α is set to 0.1. We use the mean square error for the loss function. We set the number of DRB ($N$) to 15 and the growth rate ($k$) to 32.

### 4.2 Performance comparison

The performance of our proposed network is compared with both non-CNN-based algorithms such as interpolation approaches and CNN based algorithms, respectively. The non-CNN based approaches are DLMMSE [15], DDFW [14], ESF [13], MSG [12], ARI [11], FDRI [10], MFIT [16], SOS [20], LMMSE [17] and MIFD [18] respectively. And the deep learning-based approaches are SRBF [21], CNN [22], DRL [23], GAN [24], DCNN [25], LDCN [26], RL [27], DDEMO [28] and DRDN [29] respectively. These methods are compared with the proposed method by using two subjective metrics they are structural similarity (SSIM) and color peak signal to noise ratio (CPSNR).

**JOURNAL OF ALGEBRAIC STATISTICS**
Volume 13, No. 1, 2022, p. 665-681
https://publishoa.com
ISSN: 1309-3452

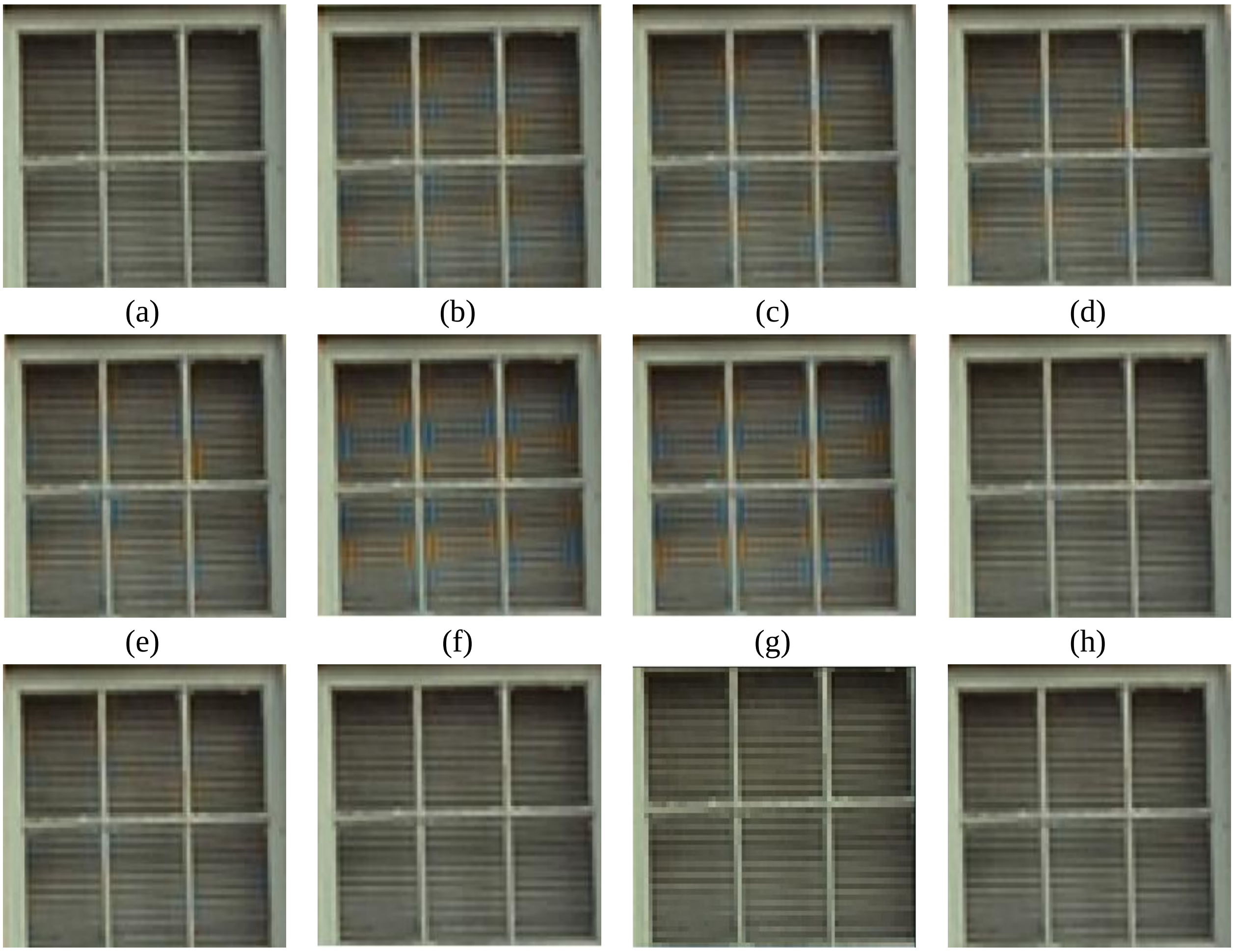

(a) (b) (c) (d)
(e) (f) (g) (h)
(i) (j) (k) (l)

**Figure 5: Demosaicked output images of various approaches. (a) Original image. (b) FDRI [10]. (c) MFIT [16]. (d) SOS [20]. (e) LMMSE [17]. (f) MIFD [18]. (g) DCNN [25]. (h) LDCN [26]. (i) RL [27]. (j) DDEMO [28]. (k) DRDN [29]. (f) proposed DRDN+ IRRGF.**

When comparing the performances of the demosaicking methods, it is important to compare whether there exist any artifacts such as zippering or false color artifacts. In Figure 5a, we compare the result images of the DIV2K dataset. As shown in the figure, the conventional demosaicking methods show false color artifacts, both with and without the CNN architecture. However, the proposed method interpolates the pixel values accurately and does not present any artifacts, respectively.Figure 6 presents the resulting images of the DIV2K dataset. As shown in the figure, the conventional methods produce false color artifacts in the form of black dots. However, the proposed method does not exhibit any false color artifacts, which establishes its excellent performance.

JOURNAL OF ALGEBRAIC STATISTICS
Volume 13, No. 1, 2022, p. 665-681
https://publishoa.com
ISSN: 1309-3452

(a) (b) (c) (d)

**Figure 6: Obtained results windows image from DIV2K dataset. (a) original image. (b) mosaicked. (c) DDEMO [28]. (d) proposed DRDN+IRRGF.**

### 4.3. Objective evaluation

Table 3 gives the detailed comparison of structural similarity (SSIM) and color peak signal to noise ratio (CPSNR) parameters for the proposed method to the state of art approaches DLMMSE [15], MIFD [18], DCNN [25], SOS [20], MFIT [16], FDRI [10], LDCN [26], DDEMO [28], DRDN [29] and DRDN + [29]. Table is listed with the comparisons of DIV2K dataset of 10 images. From the table it is observed that the proposed DRDN+ IRRGF SEM method improves the CPSNR by +1.05 dB compared to the DRDN + [29] based SEM method and improved +5dB compared to the other approaches. And the parameter SSIM also enhanced compared to the existing approaches. It means by utilizing IRRGF model with deep leaning architectures improves the demosaicking performance.

**Table 3. CPSNR and SSIM results of the proposed hybrid DRDN+ IRRGF model and existing approaches.**

| | 1 | | 2 | | 3 | | 4 | | 5 | |
|---|---|---|---|---|---|---|---|---|---|---|
| | **CPSNR** | **SSIM** | **CPSNR** | **SSIM** | **CPSNR** | **SSIM** | **CPSNR** | **SSIM** | **CPSNR** | **SSIM** |
| DLMMSE [15] | 38.962 | 0.969 | 39.41 | 0.968 | 38.27 | 0.970 | 35.14 | 0.97 | 38.82 | 0.965 |
| MIFD [18] | 35.397 | 0.969 | 37.092 | 0.960 | 33.91 | 0.971 | 39.49 | 0.922 | 39.43 | 0.968 |
| DCNN [25] | 39.152 | 0.968 | 40.37 | 0.949 | 34.39 | 0.968 | 39.20 | 0.936 | 41.54 | 0.939 |
| SOS [20] | 36.907 | 0.970 | 38.72 | 0.935 | 39.01 | 0.969 | 35.44 | 0.936 | 45.55 | 0.930 |
| MFIT [16] | 39.81 | 0.974 | 38.46 | 0.948 | 38.90 | 0.915 | 39.30 | 0.938 | 42.88 | 0.972 |

**JOURNAL OF ALGEBRAIC STATISTICS**
Volume 13, No. 1, 2022, p. 665-681
https://publishoa.com
ISSN: 1309-3452

| | | | | | | | | | | |
|---|---|---|---|---|---|---|---|---|---|---|
| FDRI[10] | 35.77 | 0.968 | 37.14 | 0.969 | 35.45 | 0.971 | 39.02 | 0.987 | 40.71 | 0.970 |
| LDCN[26] | 39.12 | 0.969 | 35.972 | 0.971 | 34.54 | 0.923 | 34.59 | 0.970 | 45.078 | 0.969 |
| DDEMO[28] | 41.91 | 0.971 | 39.19 | 0.969 | 40.57 | 0.942 | 38.09 | 0.987 | 40.17 | 0.968 |
| DRDN[29] | 42.020 | 0.973 | 38.78 | 0.980 | 41.50 | 0.989 | 42.35 | 0.983 | 43.00 | 0.969 |
| DRDN+[29] | 42.50 | 0.989 | 40.66 | 0.981 | 41.23 | 0.974 | 43.02 | 0.987 | 43.57 | 0.967 |
| **Proposed method** | **43.085** | **0.991** | **41.37** | **0.9973** | **42.46** | **0.994** | **44.56** | **0.996** | **44.23** | **0.994** |
| | 6 | | 7 | | 8 | | 9 | | 10 | |

| | **CPSNR** | **SSIM** | **CPSNR** | **SSIM** | **CPSNR** | **SSIM** | **CPSNR** | **SSIM** | **CPSNR** | **SSIM** |
|---|---|---|---|---|---|---|---|---|---|---|
| DLMMSE[15] | 37.86 | 0.987 | 35.91 | 0.980 | 42.66 | 0.984 | 41.88 | 0.9898 | 35.25 | 0.9351 |
| MIFD[18] | 38.86 | 0.989 | 39.37 | 0.979 | 38.99 | 0.976 | 38.25 | 0.9805 | 37.07 | 0.9773 |
| DCNN[25] | 41.21 | 0.979 | 31.95 | 0.980 | 39.14 | 0.974 | 37.58 | 0.9881 | 38.62 | 0.9822 |
| SOS[20] | 41.93 | 0.980 | 37.49 | 0.970 | 39.67 | 0.976 | 43.08 | 0.9589 | 40.38 | 0.9767 |
| MIFIT[16] | 38.90 | 0.979 | 40.09 | 0.978 | 40.78 | 0.984 | 35.63 | 0.9448 | 36.23 | 0.9593 |
| FDRI[10] | 39.76 | 0.981 | 36.53 | 0.976 | 37.39 | 0.988 | 36.38 | 0.9728 | 42.78 | 0.9809 |

**JOURNAL OF ALGEBRAIC STATISTICS**
Volume 13, No. 1, 2022, p. 665-681
https://publishoa.com
ISSN: 1309-3452

| | | | | | | | | | | |
|---|---|---|---|---|---|---|---|---|---|---|
| LDCN [26] | 38.81 | 0.989 | 36.89 | 0.982 | 37.06 | 0.927 | 39.69 | 0.9821 | 40.14 | 0.9099 |
| DDEMO [28] | 34.92 | 0.982 | 39.86 | 0.974 | 34.60 | 0.912 | 40.47 | 0.9864 | 36.085 | 0.8065 |
| DRDN [29] | 41.69 | 0.978 | 40.97 | 0.952 | 42.51 | 0.970 | 41.39 | 0.9380 | 40.24 | 0.9860 |
| DRDN+ [29] | 42.02 | 0.977 | 41.66 | 0.946 | 42.23 | 0.981 | 42.62 | 0.9808 | 42.79 | 0.9863 |
| **Proposed method** | **43.58** | **0.991** | **42.57** | **0.993** | **43.48** | **0.994** | **43.58** | **0.995** | **43.85** | **0.993** |

**Table 4: Objective comparison with various approaches.**

| Non-DL approaches | | | DL approaches | | |
|---|---|---|---|---|---|
| Method | CPSNR | SSIM | Method | CPSNR | SSIM |
| DLMMSE [15] | 40.11 | 0.992 | SRBF [21] | 47.46 | 0.946 |
| DDFW [14] | 40.66 | 0.991 | CNN [22] | 40.66 | 0.978 |
| ESF [13] | 40.31 | 0.974 | DRL [23] | 41.93 | 0.974 |
| MSG [12] | 40.92 | 0.982 | GAN [24] | 43.97 | 0.973 |
| ARI [11] | 39.77 | 0.957 | DCNN [25] | 40.37 | 0.967 |
| FDRI [10] | 37.77 | 0.934 | LDCN [26] | 40.04 | 0.957 |
| MFIT [16] | 41.97 | 0.947 | RL [27] | 41.33 | 0.985 |
| SOS [20] | 40.84 | 0.994 | DDEMO [28] | 42.03 | 0.947 |
| LMMSE [17] | 42.04 | 0.978 | DRDN [29] | 42.43 | 0.974 |
| MIFD [18] | 42.56 | 0.934 | DRDN + SEM [29] | 42.66 | 0.983 |
| Proposed method | 44.56 | 0.995 | Proposed method | 44.56 | 0.995 |

Table 4 compares the proposed model with various deep learning and non-deep leaning methods. Anyhow it is important thing to be analyzed that, the various authors also focused on development of Demosaicking method with non-deep learning architectures. Through, their analysis, they stated that some of non-CNN based methods gives better SSIM; CPSNR performance compared to the SEM based DCNN architectures. From the DLMMSE [15], DDFW [14] and SOS [20] approaches it is proved that the SSIM performance is increased even number of layers are increased in DLCNN. Thus, to overcome the problem of

SEM based DLCNN approaches, the proposed method utilized the IRRGF approach, which significantly increase the performance of proposed method compared both deep learning and non-deep learning approaches, respectively.

## 5. Conclusions

In this paper, an image demosaicking method using DCNN based DRDN with IRRGFapproach is proposed, where DCNN designed using improved DRB with DRDN architecture to directly generate the initial demosaicked output images, as the DCNN architecture is trained with the various mosaic patterns with various color filters. The dense residual network including dense residual blocks with long jump connections and dense connections to overcome the problem of gradient disappearance and gradient dispersion during the network training, this can improve the discriminate ability of the network. The DCNN architecture is capable of providing the enhanced demosaicked output image with the ESPCN layer enabling SEM method. Finally, The IRRGF algorithm was applied to enchase the demosaicked output by solving the complexity problems of SEM approach with enhancement of low intensity pixels. The network was trained and tested with the DIV2K database and Comparisons among different image demosaicking methods showed that the proposed method can better eliminate artifacts in the reconstructed image and can especially better restore high-frequency features, such as edges and angles of the image.

## Conflicts of Interest

The authors declare no conflict of interest.

## Author Contributions

"Conceptualization, Chatla Raja Rao; methodology, Chatla Raja Rao; software, Chatla Raja Rao; validation, Chatla Raja Rao, and Soumitra Kumar Mandal; formal analysis, Chatla Raja Rao; investigation, Chatla Raja Rao; writing—original draft preparation, Chatla Raja Rao; writing—review and editing, Chatla Raja Rao, and Soumitra Kumar Mandal;

## References

[1] K. E. Paul, V. S. Saraswathibai. Maximum accurate medical image demosaicing using WRGB based newton gregory interpolation method. *Measurement.* vol. 135, pp. 935-942, 2019.

[2] R. Zhou, R. Achanta, S. Süsstrunk. Deep residual network for joint demosaicing and super-resolution. *Color and Imaging Conference*. vol. 2018, no. 1, Society for Imaging Science and Technology, 2018.

[3] Y. Park, S. Lee, B. Jeong, J. Yoon. Joint demosaicing and denoising based on a variational deep image prior neural network. *Sensors.* vol. 20, no. 10, p. 2970, 2020.

[4] Q. Bammey, R. G. von Gioi, J. M. Morel. Reliable demosaicing detection for image forensics. *2019 27th European Signal Processing Conference (EUSIPCO)*. IEEE, 2019.

[5] N. Le, F. Retraint. An improved algorithm for digital image authentication and forgery localization using demosaicing artifacts. *IEEE Access*, vol. 7, pp. 125038-125053.

[6] T. Cover, P. Hart. Nearest neighbor pattern classification. IEEE Trans. Inf. Theory, vol. 13, no. 1, pp. 21–27, Jan. 1967.

[7] K. T. Gribbon, D. G. Bailey. A novel approach to real-time bilinear interpolation. in Proc. 2nd IEEE Int. Workshop Electron. Design, Test Appl. (DELTA), Jan. 2004, pp. 126–131.

**JOURNAL OF ALGEBRAIC STATISTICS**
Volume 13, No. 1, 2022, p. 665-681
https://publishoa.com
ISSN: 1309-3452

[8] R. G. Keys. Cubic convolution interpolation for digital image processing. IEEE Trans. Acoust., Speech, Signal Process., vol. 29, no. 6, pp. 1153–1160, Dec. 1981.

[9] R. A. Maschal, S. S. Young, J. Reynolds, K. Krapels, J. Fanning, T. Corbin. Review of Bayer pattern CFA demosaicing with new quality assessment algorithms. Proc. SPIE, vol. 7662, p. 766215, Apr. 2010.

[10] Y. Kim, J. Jeong. Four-direction residual interpolation for demosaicking. IEEE Trans. Circuits Syst. Video Technol., vol. 26, no. 5, pp. 881–890, May 2016.

[11] Y. Monno, D. Kiku, M. Tanaka, M. Okutomi. Adaptive residual interpolation for color image demosaicking. in Proc. IEEE Int. Conf. Image Process. (ICIP), Sep. 2015, pp. 3861–3865.

[12] I. Pekkucuksen, Y. Altunbasak. Multiscale gradients-based color filter array interpolation. IEEE Trans. Image Process., vol. 22, no. 1, pp. 157–165, Jan. 2013.

[13] I. Pekkucuksen, Y. Altunbasak. Edge strength filter-based color filter array interpolation. IEEE Trans. Image Process., vol. 21, no. 1, pp. 393–397, Jan. 2012.

[14] Z. Dengwen, S. Xiaoliu, D. Weiming. Colour demosaicking with directional filtering and weighting. IET Image Process., vol. 6, no. 8, pp. 1084–1092, Nov. 2012.

[15] D. Zhang, X. Wu. Color demosaicking via directional linear minimum mean square-error estimation. IEEE Trans. Image Process., vol. 14, no. 12, pp. 2167–2178, Dec. 2005.

[16] S. Tabassum, S. C. Gowre. Demosaicing using MFIT (matrix factorization iterative tunable) based on convolution neural network. *International Conference on Intelligent Data Communication Technologies and Internet of Things*. Springer, Cham, 2019, pp. 255-264.

[17] P. Amba, D. Alleysson. LMMSE Demosaicing for multicolor CFAs. *Color and Imaging Conference*. vol. 2018, no. 1, Society for Imaging Science and Technology, 2018.

[18] A. Singh, G. Singh, K. Singh. A Markov based image forgery detection approach by analyzing CFA artifacts. *Multimedia Tools and Applications*, vol. 77, no. 21, pp. 28949-28968, 2018.

[19] H. Kim, S. Lee, M. G. Kang. Demosaicing of RGBW Color Filter Array Based on Rank Minimization with Colorization Constraint. *Sensors*, vol. 20, no. 16, p. 4458, 2020.

[20] G. Singh, K. Singh. Digital image forensic approach based on the second-order statistical analysis of CFA artifacts. *Forensic Science International: Digital Investigation*, vol. 32, p. 200899, 2020.

[21] V. N. V. S. Prakash, K. S. Prasad, T. J. C. Prasad. Color image demosaicing using sparse based radial basis function network. *Alexandria Engineering Journal*, vol. 56, no. 4, pp. 477-483, 2017.

[22] S. Din, A. Paul, A. Ahmad. Lightweight deep dense Demosaicking and denoising using convolutional neural networks. *Multimedia Tools and Applications*, pp. 1-21, 2020.

[23] R. Tan, K. Zhang, W. Zuo, L. Zhang. Color image demosaicking via deep residual learning. in Proc. IEEE Int. Conf. Multimedia Expo (ICME), Jul. 2017, pp. 793–798.

[24] J. Luo, J. Wang. Image demosaicing based on generative adversarial network." *Mathematical Problems in Engineering*, 2020.

[25] V. Prakash, K. S. Prasad, T. J. C. Prasad. Deep learning approach for image denoising and image demosaicing. *International Journal of Computer Applications*, vol. 168, no. 9, pp. 18–26, 2017.

[26] N. S. Syu, Y. S. Chen, Y. Y. Chuang. Learning deep convolutional networks for demosaicing. *arXiv preprint arXiv:1802.03769* (2018).

[27] Y. Guo, et al. "Residual learning for effective joint demosaicing-denoising. *arXiv preprint arXiv:2009.06205* (2020).

[28] D. S. Tan, W.-Y. Chen, K.-L. Hua. DeepDemosaicking: Adaptive image demosaicking via multiple deep fully convolutional networks. IEEE Trans. Image Process., vol. 27, no. 5, pp. 2408–2419, May 2018.

[29] B. Park, J. Jeong. Color filter array demosaicking using densely connected residual network. *IEEE Access*, vol. 7, pp. 128076-128085, 2019.

[30] K. He, X. Zhang, S. Ren, J. Sun. Deep residual learning for image recognition. in Proc. IEEE Conf. Comput. Vis. Pattern Recognit. (CVPR), Jun. 2016, pp. 770–778.

[31] G. Huang, Z. Liu, L. van der Maaten, K. Q. Weinberger. Densely connected convolutional networks. in Proc. IEEE Conf. Comput. Vis. Pattern Recognit. (CVPR), Jul. 2017, pp. 2261–2269.

[32] Y. Zhang, Y. Tian, Y. Kong, B. Zhong, Y. Fu. Residual dense network for image super-resolution. in Proc. IEEE Conf. Comput. Vis. Pattern Recognit. (CVPR), Jun. 2018, pp. 2472–2481.

[33] W. Shi, J. Caballero, F. Huszar, J. Totz, A. P. Aitken, R. Bishop, D. Rueckert, Z. Wang. Real-time single image and video super resolution using an efficient sub-pixel convolutional neural network. in Proc. IEEE Conf. Comput. Vis. Pattern Recognit. (CVPR), Jun. 2016, pp. 1874–1883.

[34] A. Ignatov et al. “PIRM Challenge on Perceptual Image Enhancement on Smartphones: Report.” In: Leal-Taixé L., Roth S. (eds) Computer Vision – ECCV 2018 Workshops. Lecture Notes in Computer Science, vol 11133. Springer, Cham, 2019.